CHEMISTRY OF MATERIALS

ARTICLE

pubs.acs.org/cm

Influence of Polyamines and Related Macromolecules on Silicic Acid Polycondensation: Relevance to "Soluble Silicon Pools"?

Katrin Spinde,[†] Konstantinos Pachis,[‡] Ioanna Antonakaki,[‡] Silvia Paasch,[†] Eike Brunner,*[,†] and Konstantinos D. Demadis*[,‡]

[†]Fachrichtung Chemie und Lebensmittelchemie, Bioanalytische Chemie, Technische Universität Dresden, 01062 Dresden, Germany

[‡]Crystal Engineering, Growth & Design Laboratory, Department of Chemistry, University of Crete, Voutes Campus, Heraklion, Crete GR-71003, Greece

Supporting Information

ABSTRACT: The influence of a number of N-containing macromolecules on the polycondensation of silicic acid to form amorphous silica is studied by the combined use of ^{29}Si NMR spectroscopy and the silicomolybdate test. Polymeric additives include poly(allylamine hydrochloride) (PAH), the poly(aminoamide) dendrimer of generation 1 (PAMAM-1), poly(ethyleneimine) (PEI), and poly(vinylpyrrolidone) (PVP). These studies were performed under biologically relevant conditions (pH 5.4 and 7.0) using aqueous solutions of isotope-labeled sodium [^{29}Si]metasilicate as the precursor compound. It was found at pH 5.4 that all additives accelerate silicic acid polycondensation, except for PVP, which exerts a minor silicic acid stabilizing effect. At pH 7.0, polycondensation is much faster in the presence of PAMAM-1, PEI, and PAH. However, PVP significantly stabilizes mono- and disilicic acid. Silica precipitates were also studied by ^{29}Si NMR spectroscopy. The effect observed for PVP is striking and indicates that the silicic acid polycondensation is slowed, although the oligomers are immobilized by the PVP polymer. In contrast, the charged PAH attracts the oligomeric species and enhances the silicic acid polycondensation.

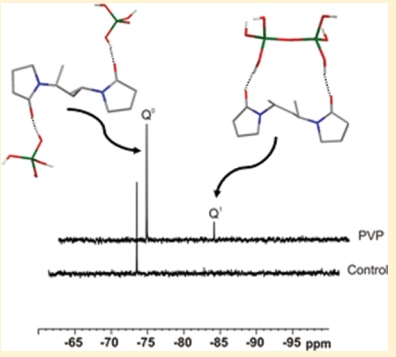

KEYWORDS: ^{29}Si NMR, silicomolybdate test, polyamines, silicic acid polycondensation, silicic acid stabilization

INTRODUCTION

The uptake, internal storage, transport, and processing of silicic acid by living organisms during biosilicification events are rewarding topics with respect to fundamental research as well as biomimetic silica synthesis approaches. Diatoms[1] are particularly interesting model systems for the study of silica biomineralization processes and as a source of inspiration for biomimetics.[2] Other biosilica-forming organisms are sponges[3−5] and plants.[6−8]

Many diatoms preferentially take up Si as monosilicic acid[9,10] ($Si(OH)_4$) via special silicon transport (SIT) proteins.[11] Active transport is necessary because the concentration of silicic acid in natural waters is often low.[12] The regulatory levels of silicon transport proteins, together with their transport activity, were recently studied on synchronized *Thalassiosira pseudonana* cultures.[13] Maximum Si uptake rates were observed during cell wall formation. These kinetics studies of various diatom species revealed that the SIT proteins determine Si uptake at low $Si(OH)_4$ concentrations. In contrast, the uptake is diffusion-controlled at high $Si(OH)_4$ levels.[14] However, the intracellular Si processing, transport, and transfer into the silica deposition vesicle (SDV) are rather poorly understood.[15,16] Numerous publications report the existence of intracellular Si storage pools in diatoms representing intracellular concentrations of ca. 19−340 mM depending on the species.[17−21] Silicon storage pools in diatom cells, if present, are supposed to accumulate Si for the production of new valves.[15] The accumulated Si is then transported into the SDV where the new cell wall is synthesized. Interestingly, the reported concentrations of intracellular Si within the storage pool[19,20] sometimes strongly exceed the solubility of monosilicic acid (ca. 2 mM, pH < 9).[21] Various types of Si storage pools are discussed in the literature. It is usually assumed that Si species are stabilized by the association with some kind of organic material such as special proteins, thus forming a soluble silicic acid pool inside the cells.[22] Special silicon transport vesicles (STVs) were proposed by Schmid and Schulz.[23] The latter suggestion is based on the observation that certain cytoplasmic vesicles are fusing with the developing SDV. However, there is no evidence for the presence of Si inside the vesicles observed in diatoms yet. In contrast, Si-containing vesicles could be identified during the formation of the siliceous spicules of sponges.[24] The detection of these putative Si storage pools usually relies on the following procedure: The cells are boiled in water for 15 min.[25] Afterward, the amount of dissolved Si in the boiling solution ("soluble silica") is quantified, usually with the so-called silicomolybdate test that detects mono- and disilicic acid.[21,26,27] This procedure—especially the boiling—may, however, result in partial dissolution of oligomeric species and their backtransformation into mono- or disilicic acid species. On the other hand,

Received: April 5, 2011
Revised: September 12, 2011
Published: October 04, 2011

solid-state ^{29}Si NMR spectroscopy (^{29}Si magic angle spinning (MAS) NMR spectroscopy) allows the detection of the different Q^n group species (Q^n = $Si(OSi)_n(OH)_{4-n}$, n = 0−4).[28] It is, therefore, widely used to characterize siliceous materials.[29−31] Liquid-state ^{29}Si NMR spectroscopy (^{29}Si high-resolution (HR) NMR spectroscopy) has previously been used to study silicic acid polycondensation,[32−34] usually at concentrations in the range from 0.5 to 1.5 M due to the low natural abundance of ^{29}Si. A method for the solid-state ^{29}Si NMR spectroscopic study of pristine, frozen diatom cells without any chemical pretreatment has been developed recently.[31,35] So far, this methodology has been applied to two different diatom species, *T. pseudonana*[35] and *Ditylum brightwellii*.[36] The latter species indeed exhibits a significant amount of monosilicic acid which even exceeds its normal solubility. However, the monosilicic acid concentration was found to be considerably lower than the concentration of soluble Si detected by using the aforementioned method (boiling + silicomolybdate test). It was, therefore, concluded[35,36] that the putative "soluble Si pools" must contain significant amounts of stabilized silica particles with low polycondensation degree and not only mono- and disilicic acid.

The idea of silicic acid stabilization by organic material has meanwhile led to various in vitro investigations to characterize the influence of the biomolecules found in diatoms upon silicic acid. For example, Kinrade et al.[37] discovered by ^{29}Si NMR spectroscopy that carbohydrate-like molecules can covalently interact with silicate to form 5- and 6-coordinated stable silicon complexes. These observations may be relevant for the understanding of Si transport and intracellular stabilization because polysaccharides are indeed found to be attached to diatom biosilica.[38] They may also imply that polysaccharide-like polymers (and "small" molecules) can affect Si transport and/or condensation.[37,39−42]

Long-chain polyamines were found to be tightly attached to diatom[43,44] as well as sponge[45] biosilica. In diatoms, such polyamines are also found covalently attached to lysine residues in special proteins, so-called silaffins.[46,47] On the basis of these observations and in vitro experiments on peptides,[48,49] proteins,[50−54] and polyamines such as polyallylamine as a model, Sumper[55] proposed the presence of so-called polyamine-stabilized silica sols as silica precursor compounds. These sols remain stable over longer time periods (24 h). However, instantaneous silica precipitation can be induced from these stabilized sols as soon as they are mixed with polyamine solutions containing properly chosen counterions such as phosphate, pyrophosphate,[55,56] or strongly acidic proteins, so-called silacidins.[57] The aforementioned immediate silica precipitation was assigned to the attraction between counterions and polyamines, resulting in some form of cross-linking.[58,59] The silica species adsorbed on polyamines are brought into close contact with each other by a self-aggregation process. This, in turn, results in the observed enhanced silica formation and precipitation.

The idea of polyamine-stabilized sols was recently supported by in vitro studies of silicic acid condensation in the presence of 1-vinylimidazole.[60] Furthermore, Annenkov et al.[61] studied the interaction between poly(vinylamine) and silicic acid in solution. The formed soluble poly(vinylamine)/silica composite nanoparticles were discussed as a species relevant with respect to the aforementioned stable "silicon storage pools" in diatoms. Interestingly, amine-terminated poly(aminoamide) dendrimers[62−64] and other polymers[65−68] (at sufficiently low concentrations, e.g., 40−100 ppm) were previously shown to slow silicic acid polycondensation. Similar observations were noted for phosphonate-grafted chitosan zwitterionic derivatives.[69,70] Furthermore, an increased solubility of amorphous silica in aqueous solutions containing tiron, a catechol derivative, 4,5-dihydroxy-1,3-benzenedisulfonate, was also found. A $[Si(tiron)]^{8-}$ complex is formed in such solutions that contains a 6-coordinated Si atom surrounded by three chelating catechol ligands.[71] It is, therefore, an important issue to gain further insight into the interaction between polyamines and silicic acid species in solution at a molecular level. The aim of the present study is the detailed analysis of the influence of polyamines/polyamine-related macromolecules upon silicic acid polycondensation by the combined use of ^{29}Si NMR spectroscopy and the silicomolybdate test. These studies include poly(allylamine hydrochloride) (PAH),[72−76] poly(vinylpyrrolidone) (PVP),[77] the poly(aminoamide) dendrimer of generation 1 (PAMAM-1), and poly(ethyleneimine) (PEI)[72,73,78,79] (see Figure 1). PAH has been selected since it is a widely used long-chain model polyamine. In contrast to PAH, PVP is an uncharged long-chain polymer which, however, also finds interest for biomimetic silica syntheses.[77] PEI[72,73,78,79] and dendrimeric polyamines[80,81] have been used in previous studies and were, therefore, included in the present analyses for comparison. The experiments were performed under biologically relevant conditions (pH 5−7) using aqueous solutions of isotope-labeled sodium [^{29}Si]metasilicate as the precursor compound.

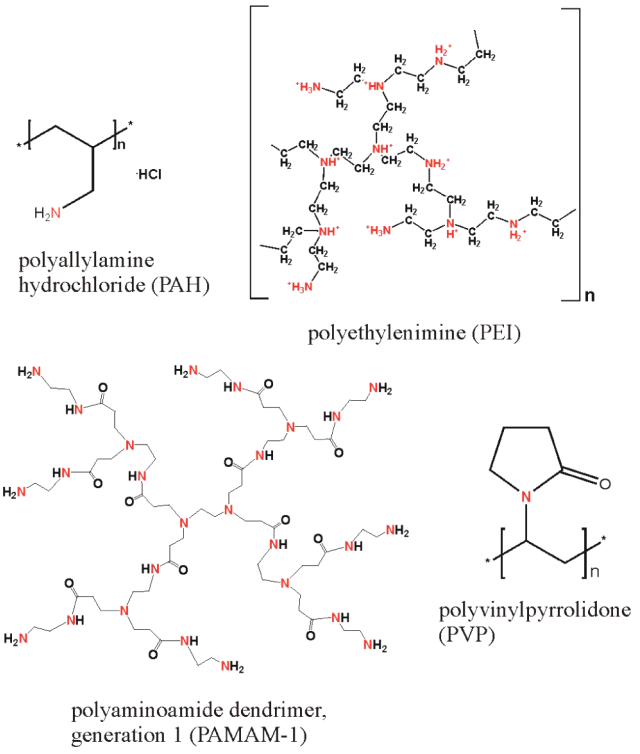

Figure 1. Schematic structures of the polymers used in this study. Nitrogen atoms are highlighted in red.

MATERIALS AND METHODS

Reagents and Chemicals. Schematic structures of the polymer additives used in this study are shown in Figure 1. PVP (MW 29 000) and PAH (MW 15 000) were purchased from Aldrich, and PEI (branched, MW 70 000, ~25% primary amines, ~50% secondary

dx.doi.org/10.1021/cm201988g |*Chem. Mater.* 2011, 23, 4676–4687

amines, and ~25% amines) was purchased from Polysciences. PAMAM-1 dendrimer was purchased from Aldrich as a 20% (w/v) solution in methanol (PAMAM-1 as well as other related dendrimers are available under the commercial name STARBURST polymers). Sodium metasilicate ($Na_2SiO_3 \cdot 5H_2O$) was obtained from EM Science (Merck) and $^{29}SiO_2$ from CortecNet (France). Ammonium molybdate ($(NH_4)_6Mo_7O_{24} \cdot 4H_2O$) and oxalic acid ($C_2H_2O_4 \cdot 2H_2O$) were purchased from EM Science (Merck), sodium hydroxide (NaOH) was purchased from Merck, and hydrochloric acid (37%) was purchased from Riedel de Haen. Acrodisc filters (0.45 μm) were obtained from Pall-Gelman Corp. In-house, nanopure water was used for all experiments. It was analyzed and found to contain only negligible amounts of soluble silica.

Synthesis of Isotope-Labeled Sodium Metasilicate. The ^{29}Si-enriched samples were prepared using 96.74% ^{29}Si-enriched sodium metasilicate ($Na_2{}^{29}SiO_3$). To obtain the latter compound, $^{29}SiO_2$ was melted with sodium carbonate (Fluka), thus forming $Na_2{}^{29}SiO_3$ in a solid-state reaction.[82] The completeness of this reaction could be monitored by ^{29}Si MAS NMR spectroscopy (see the Supporting Information, Figure S-0).

Preparation of Molybdenum Blue Test Reagents. The following solutions were prepared for the molybdenum blue spectrophotometric test: (a) 3.1 g of ammonium molybdate tetrahydrate (Sigma-Aldrich, Germany) dissolved in 50 mL of 1.0 M sulfuric acid; (b) 6.3 g of oxalic acid dihydrate (Sigma-Aldrich), and (c) 1.76 g of ascorbic acid, each dissolved in 50 mL of nanopure water.

Preparation of Sodium Silicate Solutions. The sodium silicate stock solution containing 600 ppm SiO_2 was prepared from 3.6 mg of $Na_2{}^{29}SiO_3$ dissolved in 3 mL of D_2O/H_2O (1:2). The solution was treated for 3 min in an ultrasonic bath to ensure that all the sodium metasilicate was completely dissolved. Stock solutions of the additives in water were prepared in the following concentrations: 56600 ppm PAH, 60800 ppm PAMAM-1, 25900 ppm PEI, and 66300 ppm PVP.

Silicic Acid Polycondensation Studies. A volume of 3 mL of the 600 ppm $Na_2{}^{29}SiO_3$ stock solution was placed in a glass container with a Teflon-covered magnetic stir bar. A 50 μL volume of nanopure water (control sample) or of a polymeric additive-containing stock solution was admixed. The concentrations in the additive-containing stock solutions were chosen such that the final ratio between silicon and nitrogen atoms was 1:1 (PAH, 913 ppm; PEI, 419 ppm; PAMAM-1, 995 ppm; PVP, 1082 ppm; after titration). The initial pH of this solution was 12.1. The desired pH values of 5.4 and 7.0 were adjusted by titration with a 2.4 M HCl stock solution. The volume change caused by this titration was ~3%. The resulting solution was transferred into a 10 mm NMR glass probe or—for the molybdenum blue test—placed in an Eppendorf vial. The kinetics of silicic acid polycondensation was studied by liquid-state ^{29}Si NMR spectroscopy as well as the molybdenum blue test at sampling times of 2 and 24 h after titration. For detailed investigations of stabilized silicic acid by PVP, a control and a sample with PVP were prepared. Therefore, 100 mL from a 600 ppm (as SiO_2) Na_2SiO_3 stock solution (pH ≈ 11.8) was pH-adjusted to 7.00 ± 0.01 or 5.40 ± 0.01 by addition of HCl or NaOH under continuous stirring using a poly(ethylene terephthalate) (PET) container with a Teflon-covered magnetic stir bar. If needed, the volume changes were taken into account in the calculations. After titration the container was covered with Parafilm and set aside without stirring. For short-term experiments—every hour for the first 8 h—and for long-term experiments—24, 48, and 72 h—after titration the solutions were checked for soluble silicic acid using the silicomolybdate yellow test as follows: the same procedure, but including various amounts (40, 60, 80, 100, 120, 140, and 160 ppm) of PVP, was repeated.

Determination of Soluble (Reactive) Silica. According to the established protocol, 75 μL of ammonium molybdate stock solution (a) was mixed with a 1.5 mL diluted test sample and equilibrated for 10 min after mixing. Then 75 μL of the oxalic acid solution (b) and, after 1 min, 75 μL of the reducing agent (ascorbic acid, c) solution were added to it. The resulting final solution was equilibrated for further 10 min before the absorbance was measured at 810 nm. The measurements of the molybdenum blue test were performed on a Varian Cary Scan 50 spectrophotometer. Alternatively, the silicomolybate yellow test can be used, according to the following procedure: A 2 mL volume of the filtered sample (0.45 μm syringe filter) was diluted to 25 mL in a special cylindrical cell (cell volume 25 mL). To the diluted sample, 1 ml of ammonium molybdate stock solution and 0.5 ml of 1 + 1 HCl were added, and the resulting solution was shaken well and left undisturbed for 10 min. Then 1 mL of oxalic acid solution was added and the resulting solution shaken again. After the second time period of 2 min, the absorbance at 452 nm was measured to determine the concentration as "parts per million soluble silica" using water as a blank. The measurements of molybdate-reactive silica were run on a Hach 890 spectrophotometer from the Hach Co., Loveland, CO, U.S.A.

Sample Preparation for ^{29}Si HR NMR and MAS NMR at Higher Silicic Acid Concentration. For liquid-state and solid-state ^{29}Si NMR measurements, 25.6 mg of $Na_2{}^{29}SiO_3$ was dissolved in 2 mL of D_2O/H_2O (1:1) and placed in a container with a Teflon-covered magnetic stir bar, resulting in a 6030 ppm SiO_2 stock solution. For the control sample, 800 μL of nanopure water was added, thus giving a 4500 ppm SiO_2 solution. The pH was adjusted with the 2.4 M HCl stock solution to 5.4 ± 0.1. The final concentration of silicic acid was 4200 ppm. The additive-containing samples were also prepared from the aforementioned silica stock solution (6030 ppm). Additive-containing stock solutions were admixed. After titration with 2.4 M HCl to pH 5.4, a final silicic acid concentration of 4200 ppm was obtained for all samples, and the ratio between silicon and nitrogen atoms was always kept at 1:1 (PAH, 6560 ppm; PVP, 7770 ppm). The kinetics of silicic acid polycondensation was studied by liquid-state ^{29}Si NMR. After a reaction time of 24 h, the obtained gel/precipitates were characterized by solid-state ^{29}Si NMR.

^{29}Si NMR Spectroscopy. ^{29}Si NMR experiments were performed on a Bruker Avance 300 spectrometer operating at a resonance frequency of 59.63 MHz. For liquid-state ^{29}Si NMR measurements a commercial 10 mm HR probe (56° flip angle, number of scans 180, 60 s repetition time) was used. Typical T_1 values for samples in solution were 8−13 s. Waltz16 ^{1}H decoupling was applied during signal acquisition. The chemical shift was referenced relative to tetramethylsilane (TMS), and the quantitative measurements were calibrated using a 4740 ppm sodium metasilicate solution at pH 12.8 as an external standard. ^{29}Si MAS NMR measurements were carried out on commercial double-resonance 4 mm and 2.5 mm MAS NMR probes (90° flip angle; number of scans 8000 (cross-polarization, CP), 2000 (single pulse, SP); repetition time 5 s (CP), 20 s (SP); sample spinning rate 12 kHz for the 4 mm probe, 16 kHz for the 2.5 mm probe). Typical T_1 values for samples centrifuged into the rotors are: 2−4 s for ^{29}Si and less than 1 s for ^{1}H. SPINAL64 ^{1}H decoupling[83] was applied during signal acquisition. The intensity ratios of Q^2 to Q^3 to Q^4 of the ^{29}Si MAS NMR spectra were calculated by using the program dmfit (current version dmfit#20100301).[84]

Scanning Electron Microscopy. Scanning electron microscopy (SEM) images were taken on a ZEISS DSM 982 Gemini using a 1.0 kV accelerating voltage.

RESULTS AND DISCUSSION

The polycondensation of silicic acid into amorphous silica is a spontaneous process which depends on various parameters, in particular on the silicic acid concentration[85] and pH value.[86] The highest rate of polycondensation is found around pH 7.[86] In contrast, silicic acid solutions (in the form of silicate) are stable (i.e., no polycondensation is occurring) at pH > 12 even at high concentrations (see the Supporting Information). Diatom cell

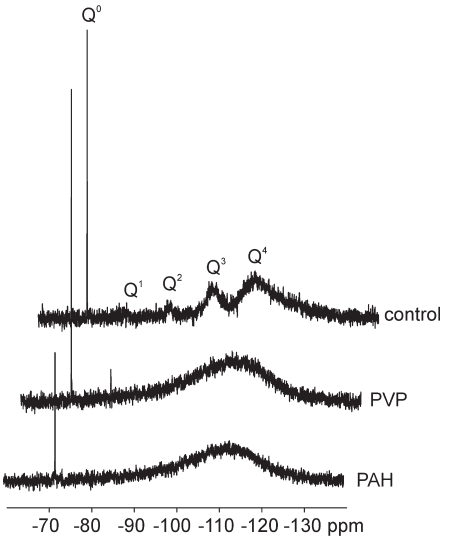

Figure 2. Background-corrected ^{29}Si HR NMR spectra of silicic acid solutions (4200 ppm) 4 h after titration at pH 5.4 in the absence or presence of PVP or PAH. The background correction is demonstrated in the Supporting Information (Figure S-5).

wall formation takes place in the SDV with an internal pH of 5−6.[87] Therefore, we have chosen two pH regions. The first was 5.4 ± 0.1. For comparison, a number of experiments were also carried out at 7.0 ± 0.1, where the maximum of the silicic acid polycondensation rate is found.

In our first experiment, we have chosen a silicic acid concentration of ∼4200 ppm at pH 5.4 and monitored its polycondensation behavior in the presence/absence of a charged (PAH) and an uncharged (PVP) polymeric additive. The results are shown in Figure 2. All three spectra exhibit the signal due to monosilicic acid (Q^0). The highest intensity of this signal is found for the PVP-containing sample. This sample also exhibits the signal due to disilicic acid (Q^1). The additive-free control sample exhibits a Q^0 signal intensity which is comparable to but somewhat smaller than that in the PVP-containing sample. Obviously, the uncharged PVP results in a slightly lower degree of polymerization of the "soluble" silicic acid species ($Q^0 + Q^1$) than the additive-free control at pH 5.4. In contrast to PVP, the charged polymer PAH results in a considerably lower concentration of soluble silicic acid, i.e., an increasing degree of polymerization. A corresponding behavior is also found at lower initial silicic acid concentration (600 ppm SiO_2; see below).

Furthermore, the additive-free control spectrum in Figure 2 exhibits the well-known signals due to Q^2, Q^3, and Q^4. The signals are significantly broadened but still resolved. In contrast, both additive-containing samples exhibit only a very broad and unresolved signal centered at −110 ppm. This observation strongly suggests that both additives result in an additional immobilization of the oligomeric Si species compared to the control. For PAH, this behavior is expected because the positively charged PAH molecules should strongly interact with the negatively charged silicic acid oligomers or small silica particles. Several studies on the acid−base behavior of silica particles prove that silica is negatively charged at pH 5.4.[88]

This means that the nanoparticles observed in the so-called polyamine-stabilized sols[55,60,61] are obviously formed by the attraction between the charged polyamines and higher silica oligomers. However, the uncharged PVP apparently exhibits a

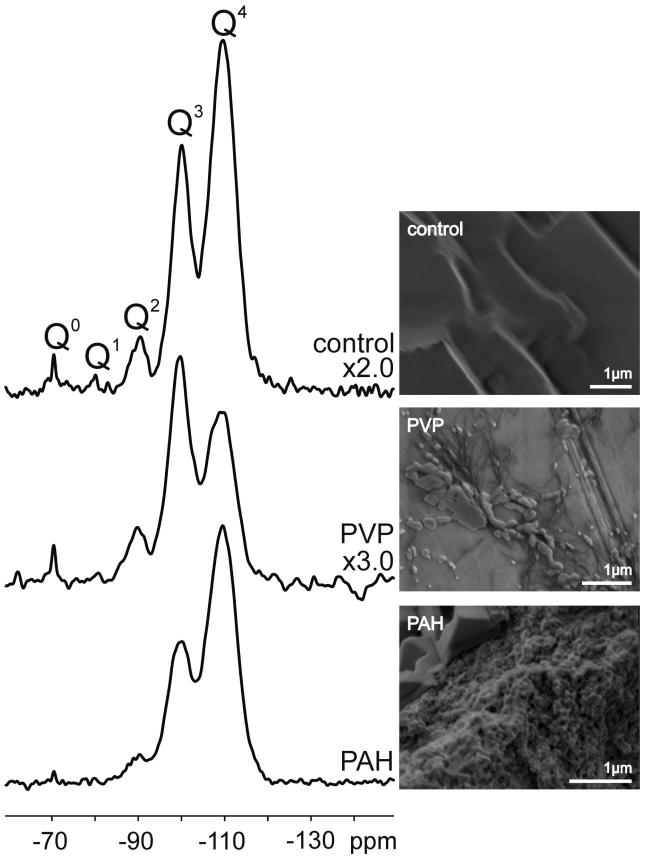

Figure 3. ^{29}Si MAS NMR spectra (SP) of silica precipitates obtained from a solution of 4200 ppm silicic acid 24 h after titration at pH 5.4 in the absence (control) or presence of polymeric additives. The SEM images of the silica precipitates obtained in the presence of polymeric additives are shown for comparison. The additive-free control is also shown and was prepared by drying the gel formed after 24 h.

similar silica−polymer association effect. Therefore, the question arises of whether this immobilization of the silicic acid oligomers is accompanied by an enhanced degree of silica polycondensation, which would be reflected by an increase in Q^4 and a simultaneous decrease in Q^3 and Q^2 signals. Unfortunately, ^{29}Si HR NMR spectroscopy cannot address this question because the corresponding signals are broadened and could only be resolved in the control.

To determine the degree of silicic acid polycondensation, we have studied silica precipitates resulting from various polycondensation experiments. At low concentrations (600 ppm) of SiO_2 and pH 5.4, silica precipitation occurs only in solutions containing PAMAM-1. Therefore, we have continuously increased the silicic acid concentrations. Beyond 1000−1200 ppm, all solutions except for the additive-free control exhibit formation of silica precipitates. The onset of precipitation was found to depend on the pH. The charged long-chain polyamines PAH and PEI start to precipitate silica below a pH of ca. 11−10.5. For the dendrimer PAMAM-1, precipitation occurs below pH 10. In the presence of the uncharged polymer PVP, precipitation is observed below pH 8.

One- and two-dimensional (1D, 2D) solid-state ^{29}Si NMR spectroscopy is a well-established tool for the study of silica as well as silica/polymer interfaces.[30,89] Figure 3 shows the ^{29}Si MAS NMR spectra and SEM images of characteristic precipitates

Table 1. Relative Intensities of the Q^2, Q^3, and Q^4 Signals Observed in ^{29}Si MAS NMR Spectra (Cf. Figure 3) of Samples Centrifuged into MAS Rotors without Drying[a]

	control			PVP			PAH		
	Q^2	Q^3	Q^4	Q^2	Q^3	Q^4	Q^2	Q^3	Q^4
relative intensity	0.1	0.5	1.0	0.1	1.0	1.0	0.1	0.4	1.0
CP/SP	0.7	0.8	0.2	2.5	2.7	1.2	0.3	0.3	0.1

[a] The relative intensity of Q^4 is normalized to 1. CP/SP denotes the intensity ratio between the absolute signal intensities observed in cross-polarization (CP) and single-pulse (SP) excited experiments on identical samples.

obtained for the PAH- and PVP-containing samples. For comparison, the control sample, i.e., pure silica gel, is shown. The SEM images were taken on dried samples. The control sample consists of unstructured plain silica blocks as a result of the slow silica polycondensation. In contrast, the presence of PAH (4200 ppm SiO_2) results in the formation of large amorphous aggregates of SiO_2 nanoparticles. This characteristic morphology is possibly due to the rapid polyamine-mediated attraction of silica species and their polycondensation, resulting in the formation of the observed nanoparticle aggregates. In the case of PAH some large particles with smooth faces also appear. Similar particles are observed in the SEM images of the control experiments. In contrast, silica precipitates containing PVP have a very different morphology characterized by fibrous structures without larger particles or superstructures. It may be that these fibrous structures represent PVP molecules or bundles of molecules covered by rather thin silica layers. The ^{29}Si MAS NMR spectra were measured on the wet precipitates/gel centrifuged into the MAS rotor. The parameters derived from the ^{29}Si MAS NMR spectra are summarized in Table 1. Notably, the polycondensation degree of the silica in the PVP-containing sample is even lower than that of the control, whereas the PAH-containing sample has a higher degree of silica polycondensation as reflected by the relative intensities of the Q^2, Q^3, and Q^4 signals (see Table 1). That means the presence of PVP at pH 5.4 does not only result in a slightly enhanced concentration of mono- and disilicic acid in the solutions as detected in the ^{29}Si HR NMR spectra (see Figure 2). It even slows the polycondensation reaction, thus giving rise to a considerably lower Q^4:Q^3 ratio than in the control. The effect observed for PVP is striking and indicates again that the silicic acid polycondensation is slowed, although the oligomers in solution are obviously attracted by the polymer (see Figure 2). In contrast, the charged PAH attracts the oligomers and accelerates the silicic acid polycondensation.

$^{29}Si\{^1H\}$ CP MAS NMR spectroscopy (see Figure 4) reveals further interesting differences between the three samples studied in Figure 2 and Table 1. The CP intensities of the three samples are significantly different. Q^0 and Q^1 signals could not be observed at all. Most likely, this is due to the high mobility of the small Q^0 and Q^1 species. It is well-known that the CP efficiency drops for mobile species. Maximum CP from ^1H to ^{29}Si is observed for the PVP-containing sample, whereas the PAH-containing sample exhibits the lowest CP effect (see Table 1). This behavior is likely due to the fact that the PAH-containing sample exhibits highly condensed silica with a smaller amount of embedded ^1H species such as hydroxyl groups/water and ^1H nuclei located at PAH molecules.

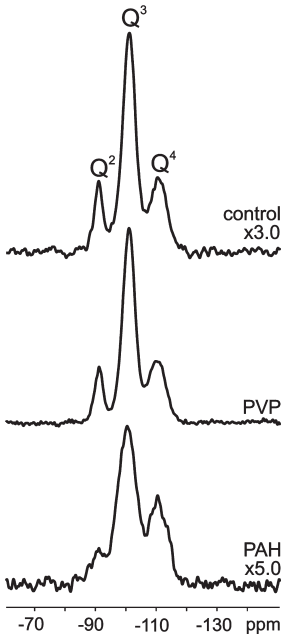

Figure 4. $^{29}Si\{^1H\}$ CP MAS NMR spectra (8000 scans, mixing time 5 s) of pure silica (control) and PVP- and PAH-containing samples 24 h after titration (pH 5.4, 4200 ppm SiO_2) centrifuged into MAS rotors. Note the pronounced intensity differences indicative of the different CP efficiencies (see Table 1).

The CP intensity in the less condensed control is somewhat higher due to the presence of a higher number of ^1H species such as OH groups and/or adsorbed water. The PVP-containing sample with its low degree of silica polycondensation exhibits the highest CP intensity. Note that no indication of 5- or 6-fold-coordinated Si species could be observed in the ^{29}Si MAS/CP MAS NMR spectra of the samples under study.

The silicic acid stabilizing effect of the uncharged PVP could also be confirmed by measurements carried out at lower silicic acid concentrations. Table 2 summarizes the results of the ^{29}Si HR NMR studies combined with the molybdenum blue test carried out at pH 5.4 (600 ppm SiO_2) for all aforementioned additives as well as the control. Furthermore, two selected additives (PEI, PVP) as well as the control were also measured at pH 7. The silica concentrations corresponding to $Q^0 + Q^1$ determined by quantitative ^{29}Si HR NMR are reproducible and in excellent agreement with those determined by the molybdenum blue test. All the charged additives (PAH, PEI, and PAMAM-1) more or less enhance silicic acid polycondensation. The strongest polycondensation-enhancing effect is found for PAH and PEI. At pH 5.4, the equilibrium value is reached with both additives even within 24 h in contrast to that of the control. PAMAM-1 has a less pronounced but measurable accelerating effect. It is, however, remarkable that it still allows the presence of some disilicic acid. This may be due to the presence of uncharged amine moieties in the dendrimer (see Figure 1). In contrast to the charged additives, the uncharged PVP does not cause any enhancement of silicic acid polycondensation compared to the control.

This is also reflected by the ^{29}Si HR NMR spectra shown in Figures 5 and 6. Comparison of the PVP-containing sample and the control at pH 5.4 suggests a minor stabilization of both mono- and disilicic acid by PVP, although the effect is still on the

Table 2. Soluble Si Species (Mono- and Disilicic Acid) Determined by ^{29}Si HR NMR and by the Molybdenum Blue Spectrophotometric Test (Mo Test)

		soluble silica as mono- and disilicic acid (expressed as ppm SiO_2)							
		polycondensation time 2 h				.			
pH	additive	Q^0	Q^1	$Q^0 + Q^1$	Mo test	Q^0	Q^1	$Q^0 + Q^1$	Mo test
5.4	control	309	45	354	371	302	41	343	317
	PVP	371	67	438	434	343	54	396	362
	PAMAM-1	281	42	323	325	247	30	277	235
	PEI	188	6	194	197	145		145	146
	PAH	173		173	156	127		127	130
7.0	control	334	48	382	356	146	5	151	164
	PVP	296	43	339	384	271	47	317	338
	PEI	150		150	157	140		140	134

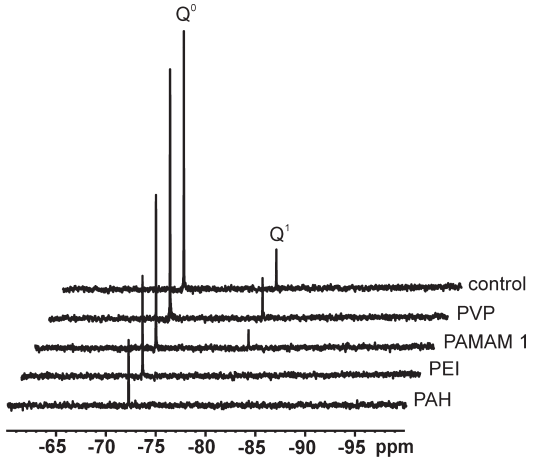

Figure 5. Background-corrected ^{29}Si HR NMR spectra of silicic acid solutions (600 ppm) 24 h after titration to pH 5.4. The samples contain either no polymeric additives (control) or polymers (as indicated) at appropriate concentrations so that the ratio between Si and N atoms is 1:1.

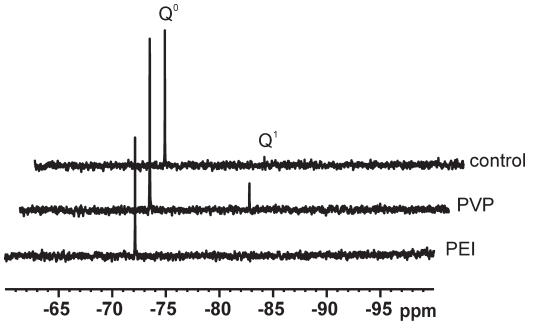

Figure 6. Background-corrected ^{29}Si HR NMR spectra of silicic acid solutions (600 ppm) 24 h after titration at pH 7. The samples contain either no polymeric additives (control) or polymers (as indicated) at concentrations corresponding to a ratio between Si and N atoms of 1:1.

order of the experimental error of 10%. However, the spectra measured at pH 7 (see Figure 6) clearly show the stabilizing effect of PVP on mono- and disilicic acid. In contrast, the charged additive PEI results in almost the same spectrum as the one observed for the control at pH 7. The main signal detected in the latter two samples is due to monosilicic acid. The control still exhibits a minor amount of Q^1. Its concentration corresponds to the aforementioned equilibrium value given by the expected solubility. This is again in excellent agreement with the molybdenum blue test results at pH 7 (see Table 2).

In summary, it can be stated that the charged additives (PAH, PEI, PAMAM-1) all enhance silicic acid polycondensation. The most pronounced effects are observed for PAH and PEI. Furthermore, they attract higher silicic acid oligomers, forming aggregates. The latter is also true for the uncharged polymer PVP. However, PVP does not accelerate silicic acid polycondensation. In contrast to the charged additives, it even stabilizes mono- and disilicic acid compared to the control, especially at pH 7. This means, the presence of such uncharged polymers may cause a "supersaturation" of silicic acid solutions. This interesting effect is further studied at different PVP levels (40−160 ppm) in the following. Two types of experiments were carried out, "short-term" (sampling every 1 h for 8 h) and "long-term" (sampling every 24 h for 3 days), at pH values of 5.4 and 7.0 chosen in the above-described experiments.

Long-Term (3 days) Silicic Acid Polycondensation in the Presence of PVP. *pH 7.0 Region.* The soluble silicic acid levels observed at pH 7 are shown in Figure 7. PVP concentrations between 40 ppm (1.38 μM) and 160 ppm (5.52 μM) were tested. The retarding effect of PVP is concentration dependent only for the 24 h measurements. At 140 ppm (4.83 μM) PVP concentration, the amount of soluble silicic acid reaches ca. 290 ppm and levels off beyond that concentration. The amount of soluble silicic acid decreases with increasing time. After 48 h, it drops to ∼190 ppm for a PVP level of 140 ppm, which is, however, still beyond that of the control (soluble silicic acid 140 ppm). After 72 h, the silicic acid level reaches 174 ppm (at 140 ppm PVP), ca. 40 ppm higher than that of the control. The soluble silicic acid levels are statistically indistinguishable between the 48 and 72 h measurements.

pH 5.4 Region. Silicic acid polycondensation at pH 5.4 is slower than that at pH 7.0. This becomes obvious from Figure 8. Both the control and PVP-containing solutions exhibit higher silicic acid levels compared to those of the corresponding experiments at pH 7.0 (see Figure 7). The inhibition of silicic acid polycondensation is again observed, although it is much less dependent on the PVP concentration. For PVP levels between

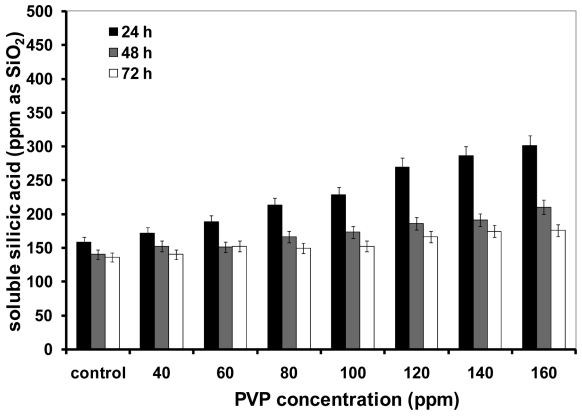

Figure 7. Concentration dependence of the condensation-retarding effect of PVP at pH 7.0 in 3 day silicic acid polycondensation experiments.

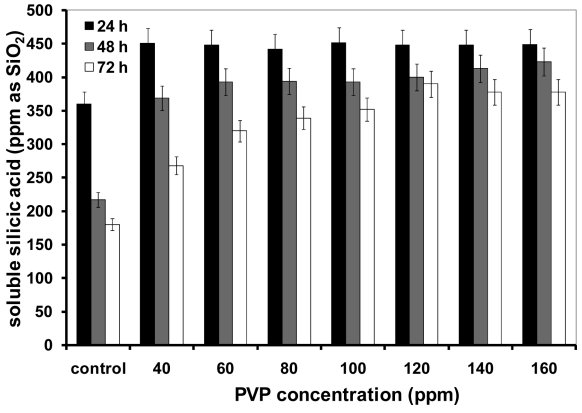

Figure 8. Concentration dependence of the condensation-retarding effect of PVP at pH 5.4 in 3 day silicic acid polycondensation experiments.

40 and 160 ppm (1.38−5.52 μM), the amount of soluble silicic acid reaches ~450 ppm after 24 h, a result that is statistically the same for all these PVP concentrations. These levels decrease over time. The drop is, however, not as strong as that for pH 7.0. Finally, the amount of soluble silicic acid after 72 h is ~390 ppm (control 180 ppm).

Short-Term (8 h) Silicic Acid Polycondensation in the Presence of PVP. *pH 7.0 Region.* The experiments shown in Figure 9 again clearly demonstrate the stabilizing effect of PVP at pH 7.0, i.e., at the maximum silicic acid polycondensation rate. A PVP concentration of 140 ppm (4.83 μM) was used. Silicic acid levels of the pure (control) and PVP-containing solutions decrease as polycondensation proceeds. After 8 h, the difference between the two samples amounts to ca. 200 ppm.

pH 5.4 Region. As stated before, silicic acid polycondensation is slower at pH 5.4. This is also reflected in the 8 h experiment shown in Figure 10: the silicic acid concentration in the control decreases much slower than that at pH 7.0 (Figure 9). PVP almost completely stabilizes uncondensed silicic acid over 8 h. At the end of the 8 h period, the difference in silicic acid levels between the two solutions amounts to ca. 180 ppm.

Possible Mechanisms of Silicic Acid Stabilization by PVP. To understand the observed stabilizing effect of PVP on silicic

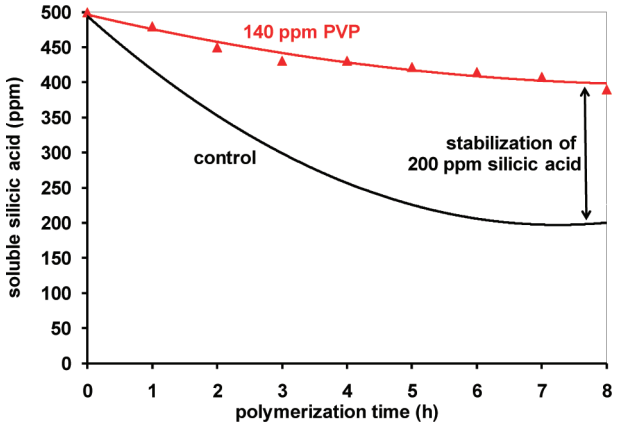

Figure 9. Condensation-retarding effect of PVP at the 140 ppm level and at pH 7.0 in an 8 h silicic acid polycondensation run.

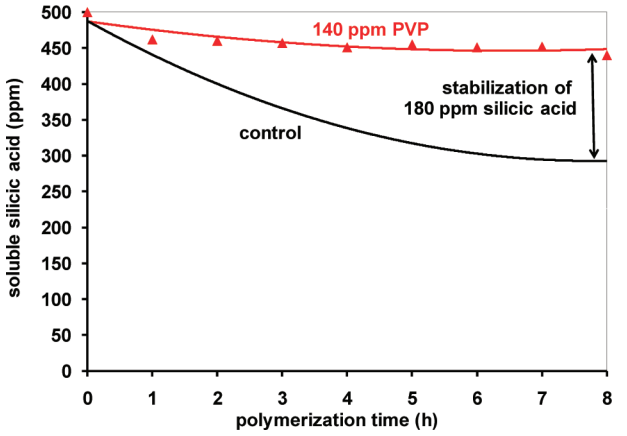

Figure 10. Condensation-retarding effect of PVP at the 140 ppm level and at pH 5.4 in an 8 h silicic acid polycondensation run.

acid, the interactions between these two species must be analyzed. The interaction of PVP with metasilicic acid in corresponding solutions has not yet been investigated to the best of our knowledge. In contrast, the interaction with silica particles has been studied previously. Robinson and Williams[90] found that PVP adsorbs onto silica particles through interaction of the carbonyl groups of the pyrrolidone rings with silanol groups on the silica surface. The adsorption capacity depends on the molecular mass of PVP but is independent of the ionic strength and pH. Belyakova et al. studied the process of adsorption−desorption of PVP onto the surface of highly dispersed amorphous silica.[91] It was shown that PVP occurs in two forms on the silica surface, reversibly adsorbed and irreversibly grafted onto the surface of silica. On the basis of FT-IR studies, the authors concluded that hydrogen bond formation takes place between the silanol groups of the silica surface and the nitrogen and/or oxygen atoms of −N—C═O groups of the adsorbed PVP (see the Supporting Information, Figure S-9). On the basis of FT-IR measurements, Gun'ko et al. suggested that the adsorption of PVP on fumed silica surfaces is due to the formation of relatively strong C═O···H—OSi hydrogen bonds.[92] Since PVP is an internal amide, N atoms are in planar conformation due to the amide bond and can only form relatively weak hydrogen bonds. It is, therefore, reasonable to assume that

dx.doi.org/10.1021/cm201988g |*Chem. Mater.* 2011, 23, 4676–4687

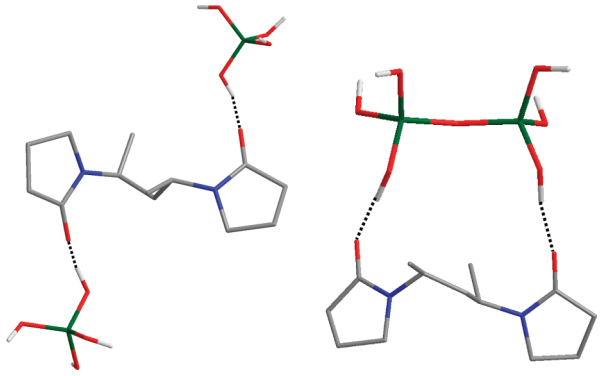

Figure 11. Schematic representations of possible hydrogen-bonding interactions between monosilicic acid (left) and disilicic acid (right) molecules with the C═O group from PVP. Color codes: C, gray; N, blue; O, red; Si, green. H atoms are omitted for clarity.

the N atoms do not participate in the interaction with the silica surfaces; i.e., it was concluded that PVP interacts with the silica surfaces via hydrogen bonding between the C═O groups and free silanols.[93] Similar results were also obtained by Hsiao and Huang studying the formation of SiO_2/PVP hybrid composites by tetraethoxysilane (TEOS) hydrolysis and condensation.[77] Xu et al. also showed that the C═O moiety is involved in hydrogen bonding with the Si−OH groups of silica particles. They, furthermore, concluded that $Si-O^{-}\cdots H^{+}$ interactions are unlikely due to the weak basicity of the N atoms in the pyrrolidone groups and the weak acidity of Si−OH groups in hydrolyzed monomers. Furthermore, ^{13}C NMR spectroscopy showed that the chemical shift of the C═O groups shifts from 179.16 to 181.47 ppm in ethanol solution, an additional indication of hydrogen-bonding interactions.[94] Solid-state ^{13}C NMR studies on PVP/silica composites[77] also reveal a shift of the C═O signal on the order of 1 ppm to higher chemical shift values. In agreement with these previous results, we have observed a shift of this signal from 176.8 to 177.4 ppm in our precipitates (see the Supporting Information, Figure S-9).

Examination of the PVP structure (see the Supporting Information, Figure S-10) confirms that there are only two potential points of interaction with silicic acid, the N and the carbonyl O. However, as mentioned before, the N atom participates in the amide bond and does not possess a lone pair for hydrogen bond interactions. As described above, the carbonyl oxygen is capable of interacting with the Si−OH of silica surfaces through hydrogen bonding. Similar interactions can be envisioned between the C═O and $Si(OH)_4$. It should be noted in this context that poly(ethyloxazoline) (PEOX), a linear, neutral, amide-containing polymer, was also found to effectively stabilize silicic acid.[95]

The structure of PVP also reveals that there are no moieties in the polymer backbone that may induce substantial folding to create "pockets" that can store more than one silicic acid molecule. Otherwise, the polymer would induce silicic acid polycondensation. The minor disilicic acid stabilization effect exerted by PVP may be explained by hydrogen-bonding interactions between disilicic acid and two vicinal C═O groups. Possible O···O distances (between two neighboring pyrrolidone monomers) are in the range of 4.5−5.6 Å, whereas the longest O···O distances in disilicic acid are 5.0−5.2 Å. Therefore, a hydrogen-bonding interaction between a disilicic acid molecule and two neighboring pyrrolidone units is possible. It should be noted that the hydrogen-bonded complexes possibly formed with mono- and disilicic acid must be short-lived because the corresponding ^{29}Si HR NMR signals remain narrow (see Figures 2, 5, and 6). Figure 11 presents a schematic depiction of these two hypothesized types of stabilization.

$^{1}H-^{29}Si$ 2D heteronuclear correlation (HETCOR) experiments were performed to further characterize the interactions between PVP and silica species in the prepared precipitates (cf. Figures 3 and 4). Frequency-switched Lee−Goldburg[96] decoupling was applied during t_1 evolution to obtain maximum spectral resolution. Since 2D measurements on the centrifuged samples were hampered by sensitivity problems, the samples had to be vacuum-dried at 40 °C. This allowed filling the MAS rotors with much higher amounts of the dried, powdered sample than by centrifugation of the wet material. On the other hand, the vacuum-drying procedure may of course be accompanied by further condensation of the silica. This is indeed observed in the 1D ^{29}Si MAS NMR spectra (see the Supporting Information, Figure S-11). However, it also becomes obvious from these spectra that the PVP-containing sample remains to be the sample with the lowest degree of silica polycondensation as was the case before drying. The investigation of the dried material is, therefore, still relevant. Figure 12 shows the $^{1}H-^{29}Si$ 2D HETCOR spectra of the additive-free control and the PVP-containing sample. The spectra exhibit remarkable differences. For the control, $^{1}H-^{29}Si$ CP transfer occurs from two distinct ^{1}H species giving rise to signals at 2.5 and 5.4 ppm. The only ^{1}H-bearing species in the control are hydroxyl groups (SiOH) and water molecules adsorbed strong enough to withstand the vacuum drying and/or readsorbed during the sample transfer into the rotor. Free or weakly hydrogen-bonded Si−OH groups typically occur at low chemical shift. The signal at 2.5 ppm is, therefore, attributed to such species. Adsorbed water typically gives resonances at around 5 ppm. The signal at 5.4 ppm is therefore likely to be due to adsorbed H_2O molecules which are not removed by the drying procedure or readsorbed (see above). In analogy to the control, the PVP-containing sample also exhibits a signal at ca. 2 ppm which can be attributed to free and/or weakly hydrogen-bonded Si−OH. Furthermore, the aliphatic ^{1}H species located at the PVP molecules can contribute to this signal. The spectral resolution is, however, insufficient to resolve the different signal contributions. Furthermore, efficient $^{1}H-^{29}Si$ CP transfer is observed from two ^{1}H species giving rise to signals at ca. 8 and 12 ppm. At a 10 ms mixing time, the signal at 8 ppm is the major source of polarization. At shorter mixing times (Figure 12, bottom), the 12 ppm signal is almost equally important as the 8 ppm signal.

^{13}C CP MAS NMR spectroscopy shows that the PVP molecules embedded into the precipitates are chemically unmodified (see the Supporting Information, Figure S-9). Since PVP only contains aliphatic ^{1}H nuclei with chemical shifts between 1 and 4 ppm,[97] the latter species must be associated with the silica. Furthermore, these species exhibit the most intense CP transfer to ^{29}Si for short CP contact times (Figure 12, bottom). That means the corresponding ^{1}H nuclei are in close proximity to the ^{29}Si nuclei. It is therefore concluded that these species are possibly due to the presence of relatively strong C═O···H—OSi hydrogen bonds as suggested earlier by Gun'ko et al.[92] Although adsorbed water usually gives rise to signals around ca. 5 ppm, an alternative explanation for the observed signals at ca. 8 and 12 ppm would be the presence of strongly adsorbed and

dx.doi.org/10.1021/cm201988g |*Chem. Mater.* 2011, 23, 4676–4687

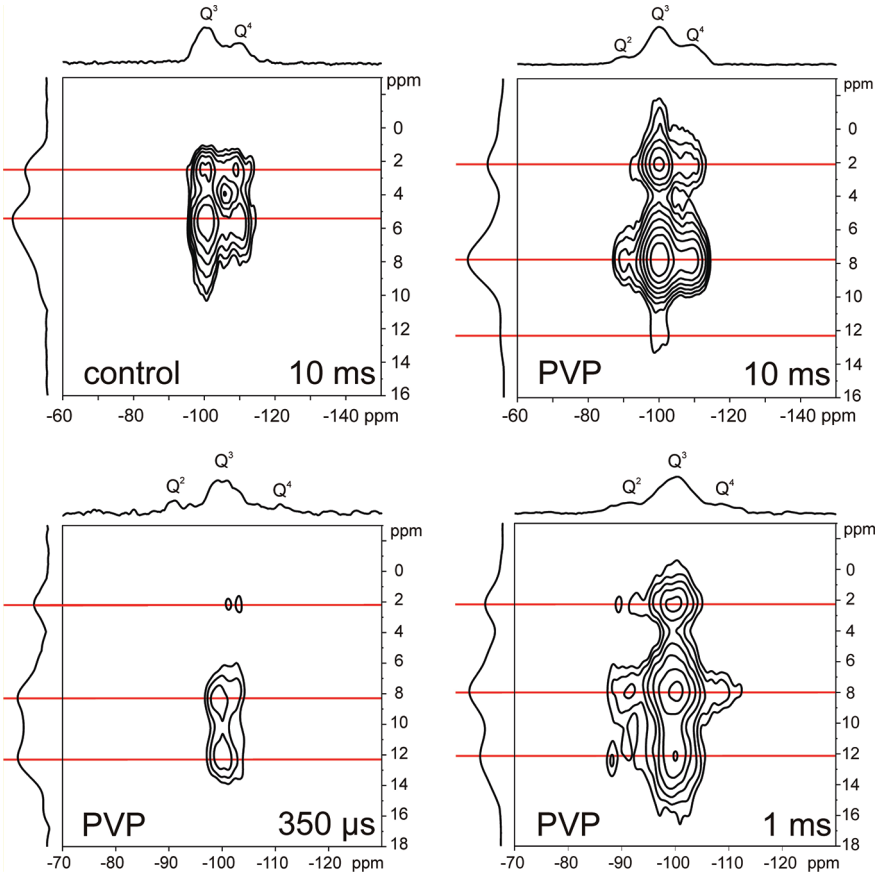

Figure 12. $^{1}H-^{29}Si$ 2D HETCOR spectra of the additive-free control (top, left) and a PVP-containing precipitate (top, right) measured with a 10 ms CP contact time and frequency-switched Lee−Goldburg decoupling during t_1 evolution. At the bottom, HETCOR spectra measured at lower contact times (left, 350 μs; right, 1 ms) for the PVP-containing precipitate are shown. These short contact times were applied to visualize the ^{1}H nuclei closely located at the ^{29}Si. The two ^{1}H species giving rise to signals at ca. 8 and 12 ppm exhibit the strongest CP transfer to ^{29}Si, indicating their close proximity to the ^{29}Si nuclei. For the control, these short contact times did not deliver spectra of sufficient quality due to the much lower CP intensity (see Table 1). The samples were vacuum-dried at 40 °C and transferred into the MAS rotor immediately.

hydrogen-bonded H_2O molecules in close proximity to the ^{29}Si nuclei. Such species are not observed in the additive-free control. If they are present, they must hence be involved in the interaction between PVP and the silica. In any case, it can be stated that the interaction between PVP and silica results in a pronounced stabilization of silica species with a lower degree of polycondensation than in the control. This is even true after vacuum drying, resulting in a powdered silica/PVP composite material of low degree of silica polycondensation. The responsible interactions involve the presence of strongly hydrogen-bonded species (SiOH or H_2O) giving rise to pronounced ^{1}H NMR signals at ca. 8 and 12 ppm.

CONCLUSIONS

Bioinspired silica chemistry relies on the transfer of biological processes into sol−gel chemistry.[98,99] Revealing the mechanisms governing biosilicification offers the prospect of developing environmentally benign routes[100,101] to synthesize new silicon-based materials and to resolve the biological use of silicon in higher organisms.[102]

The purpose of the present work was the characterization of the influence of certain macromolecular structures on silicic acid polycondensation by combining ^{29}Si NMR spectroscopy and the silicomolybdate test. Charged macromolecules such as PAH, PEI, and PAMAM-1 accelerate silica formation under the applied conditions. In contrast, PVP is able to stabilize enhanced silicic acid concentrations over longer periods of time (days). In addition to the previously described[55,60,61] polyamine-stabilized sols consisting of precondensed silica nanoparticles, the observed stabilization of soluble silicic acid by uncharged polymers may be of interest for Si transport to and storage within the diatom cell, which require relatively high Si concentrations over a certain period of time.

Major conclusions of this study are the following: Macromolecules containing amine moieties (PAMAM-1, PAH, PEI) when added at concentrations corresponding to a ratio between Si and N atoms of 1:1 enhance the polycondensation of silicic acid to form amorphous silica. This observation emphasizes the accelerating influence of charged polyamines upon silicic acid polycondensation in aqueous solutions. Using ^{29}Si isotope-labeled metasilicic acid, ^{29}Si NMR spectroscopy was proven to be a useful tool to study these effects even at relatively low concentrations. ^{29}Si HR NMR allows Q^0 and Q^1 groups to be distinguished in contrast to the silicomolybdate test, which appears to be more "promiscuous" in that regard.

PVP exerts a silicic acid stabilizing effect, especially at pH 7. It significantly stabilizes mono- and disilicic acid in contrast to

dx.doi.org/10.1021/cm201988g |Chem. Mater. 2011, 23, 4676–4687

the aforementioned behavior of the charged additives. This was established by both ^{29}Si HR NMR spectroscopy and the silicomolybdate test. In other words, the presence of uncharged, hydrogen-bond-forming polymers in solution may result in significantly higher silicic acid concentrations than predicted by the solubility in pure aqueous solutions.

It is suggested that PVP stabilizes mono- and disilicic acid through short-lived C═O···H—O—Si hydrogen bond complexes. Higher oligomers are immobilized by their interaction with the PVP polymer. Silica precipitates isolated from PVP-containing silicification experiments were studied by ^{29}Si MAS NMR spectroscopy. The effects observed for PVP support the conclusion that silicic acid polycondensation is slowed by this uncharged, hydrogen-bond-forming polymer.

■ ASSOCIATED CONTENT

Supporting Information. ^{29}Si MAS NMR of $^{29}SiO_2$ and sodium metasilicate, ^{29}Si HR NMR spectroscopy and molybdenum blue test of silicic acid solutions, demonstration of the background correction applied to the ^{29}Si HR NMR spectra, analysis of precipitated silica, SEM images of the precipitates obtained from PAMAM-1- and PEI-containing solutions, model for silica−PVP interactions, ^{13}C CP MAS NMR of PVP-containing precipitates, structure of PVP, and ^{29}Si MAS NMR of precipitates after vacuum-drying at 40 °C (PDF). This material is available free of charge via the Internet at http://pubs.acs.org.

■ AUTHOR INFORMATION

Corresponding Author

*E-mail: demadis@chemistry.uoc.gr (K.D.D.); eike.brunner@tu-dresden.de (E.B.).

■ ACKNOWLEDGMENT

E.B. gratefully acknowledges financial support by the Deutsche Forschungsgemeinschaft (Grant BR 1278/12-3). K. D.D. thanks the Special Account of Research Funding (ELKE) at the University of Crete, Grant KA 3121.

■ REFERENCES

(1) Round, F. E.; Crawford, R. M.; Mann, D. G. *The Diatoms*; Cambridge University Press: Cambridge, U.K., 1990.

(2) (a) Nassif, N.; Livage, J. *Chem. Soc. Rev.* **2011**, *40*, 849–859. (b) Bao, Z.; Ernst, E. M.; Yoo, S.; Sandhage, K. H. *Adv. Mater.* **2009**, *21*, 474–478. (c) Dickerson, M. B.; Sandhage, K. H.; Naik, R. R. *Chem. Rev.* **2008**, *108*, 4935–4978. (d) Kröger, N.; Sandhage, K. H. *MRS Bull.* **2010**, *35*, 122–125. (e) Gordon, R.; Losic, D.; Tiffany, M. A.; Nagy, S. S.; Sterrenburg, F. A. S. *Trends Biotechnol.* **2009**, *27*, 116–127. (f) Neethirajan, S.; Gordon, R.; Wang, L. *Trends Biotechnol.* **2009**, *27*, 461–467.

(3) Shimizu, K.; Cha, J.; Stucky, G. D.; Morse, D. E. *Proc. Natl. Acad. Sci. U.S.A.* **1998**, *95*, 6234–6238.

(4) (a) Müller, W. E. G.; Rothenberger, M.; Boreiko, A.; Tremel, W.; Reiber, A.; Schröder, H. C. *Cell Tissue Res.* **2005**, *321*, 285–297. (b) Schröder, H. C.; Wang, X.; Tremel, W.; Ushijima, H.; Müller, W. E. G. *Nat. Prod. Rep.* **2008**, *25*, 455–474. (c) Schröder, H. C.; Brandt, D.; Schloßmacher, U.; Wang, X.; Tahir, M. N.; Tremel, W.; Belikov, S. I.; Müller, W. E. G. *Naturwissenschaften* **2007**, *94*, 339–359.

(5) Ehrlich, H.; Deutzmann, R.; Brunner, E.; Cappellini, E.; Koon, H.; Solazzo, C.; Yang, Y.; Ashford, D.; Thomas-Oates, J.; Lubeck, M.; Baessmann, C.; Langrock, T.; Hoffmann, R.; Wörheide, G.; Reitner, J.; Simon, P.; Tsurkan, M.; Ereskovsky, A. V.; Kurek, D.; Bazhenov, V. V.; Hunoldt, S.; Mertig, M.; Vyalikh, D. V.; Molodtsov, S. L.; Kummer, K.; Worch, H.; Smetacek, V.; Collins, M. J. *Nat. Chem.* **2010**, *2*, 1084–1088.

(6) Raleigh, G. J. *Soil Sci.* **1945**, *60*, 133–136.

(7) Liou, T.-H.; Wu, S.-J. *Ind. Eng. Chem. Res.* **2010**, *49*, 8379–8387.

(8) Currie, H. A.; Perry, C. C. *Ann. Bot. (London)* **2007**, *100*, 1383–1389.

(9) Lewin, J. C. *Plant Physiol.* **1955**, *30*, 129–134.

(10) Del Amo, Y.; Brzezinski, M. A. *J. Phycol.* **1999**, *35*, 1162–1170.

(11) Hildebrand, M.; Volcani, B. E.; Gassmann, W.; Schroeder, J. I. *Nature* **1997**, *385*, 688–689.

(12) Ning, R. Y. *Desalin. Water Treat.* **2010**, *21*, 79–86.

(13) Thamatrakoln, K.; Hildebrand, M. *Eukaryotic Cell* **2007**, *6*, 271–279.

(14) Thamatrakoln, K.; Hildebrand, M. *Plant Physiol.* **2008**, *146*, 1397–1407.

(15) Hildebrand, M. In *Biomineralization—From Biology to Biotechnology and Medical Applications*; Bäuerlein, E., Ed.; Wiley: Weinheim, Germany, 2000; pp 170−188.

(16) Sumper, M.; Brunner, E. *ChemBioChem* **2008**, *9*, 1187–1194.

(17) Werner, D. *Arch. Mikrobiol.* **1966**, *55*, 278–308.

(18) Chisholm, S. W.; Azam, F.; Eppley, R. W. *Limnol. Oceanogr.* **1978**, *23*, 518–529.

(19) Martin-Jézéquel, V.; Hildebrand, M.; Brzezinski, M. A. *J. Phycol.* **2000**, *36*, 821–840.

(20) Martin-Jézéquel, V.; Lopez, P. *Prog. Mol. Subcell. Biol.* **2003**, *33*, 99–124.

(21) Iler, R. K. *The Chemistry of Silica*; Wiley: New York, 1979.

(22) Azam, F. *Planta* **1974**, *121*, 205–212.

(23) Schmid, A.-M. M.; Schulz, D. *Protoplasma* **1979**, *100*, 267–288.

(24) Schröder, H. C.; Natalio, F.; Shukoor, I.; Tremel, W.; Schloßmacher, U.; Wang, X.; Müller, W. E. G. *J. Struct. Biol.* **2007**, *159*, 325–334.

(25) Sullivan, C. W. *J. Phycol.* **1979**, *15*, 210–216.

(26) Mullin, J. B.; Riley, J. P. *Anal. Chim. Acta* **1955**, *12*, 162–176.

(27) Coradin, T.; Eglin, D.; Livage, J. *Spectroscopy* **2004**, *18*, 567–576.

(28) Engelhardt, G.; Michel, D. *Adv. Colloid Interface Sci.* **1985**, *23*, 67–128.

(29) Babonneau, F.; Baccile, N.; Laurent, G.; Maquet, J.; Azais, T.; Gervais, C.; Bonhomme, C. *C. R. Chim.* **2010**, *13*, 58–68.

(30) Engelhardt, G.; Michel, D. *High-Resolution Solid-State NMR of Silicates and Zeolites*; Wiley-VCH: Chichester, U.K., 1987.

(31) Tesson, B.; Masse, S.; Laurent, G.; Maquet, J.; Livage, J.; Martin-Jézéquel, V.; Coradin, T. *Anal. Bioanal. Chem.* **2008**, *390*, 1889–1898.

(32) Harris, R. K.; Knight, C. T. G. *J. Chem. Soc., Chem. Commun.* **1980**, 726–727.

(33) Knight, C. T. G.; Kirkpatrick, R. J.; Oldfield, E. *J. Magn. Reson.* **1988**, *78*, 31–40.

(34) Brus, J.; Karhan, J.; Koltik, P. *Collect. Czech. Chem. Commun.* **1996**, *61*, 691–703.

(35) Gröger, C.; Sumper, M.; Brunner, E. *J. Struct. Biol.* **2008**, *161*, 55–63.

(36) Brunner, E.; Gröger, C.; Lutz, K.; Richthammer, P.; Spinde, K.; Sumper, M. *Appl. Microbiol. Biotechnol.* **2009**, *84*, 607–616.

(37) Kinrade, S. D.; Hamilton, R. J.; Schach, A. S.; Knight, C. T. G. *J. Chem. Soc., Dalton Trans.* **2001**, 961–963.

(38) Chiovitti, A.; Harper, R. E.; Willis, A.; Bacic, A.; Mulvaney, P.; Wetherbee, R. *J. Phycol.* **2005**, *41*, 1154–1161.

(39) Kinrade, S. D.; Gillson, A.-M. E.; Knight, C. T. G. *J. Chem. Soc., Dalton Trans.* **2002**, 307–309.

(40) Kinrade, S. D.; Schach, A. S.; Hamilton, R. J.; Knight, C. T. G. *Chem. Commun.* **2001**, 1564–1565.

(41) Kinrade, S. D.; Balec, R. J.; Schach, A. S.; Wang, J. P.; Knight, C. T. G. *Dalton Trans.* **2004**, 3241–3243.

(42) Kinrade, S. D.; Del Nin, J. W.; Schach, A. S.; Sloan, T. A.; Wilson, K. L.; Knight, C. T. G. *Science* **1999**, *285*, 1542–1545.

(43) Kröger, N.; Deutzmann, R.; Bergsdorf, C.; Sumper, M. *Proc. Natl. Acad. Sci. U.S.A.* **2000**, *97*, 14133–14138.
(44) Sumper, M.; Brunner, E.; Lehmann, G. *FEBS Lett.* **2005**, *579*, 3765–3769.
(45) Matsunaga, S.; Sakai, R.; Jimbo, M.; Kamiya, H. *ChemBioChem* **2007**, *8*, 1729–1735.
(46) Kröger, N.; Deutzmann, R.; Sumper, M. *Science* **1999**, *286*, 1129–1132.
(47) Kröger, N.; Lorenz, S.; Brunner, E.; Sumper, M. *Science* **2002**, *298*, 584–586.
(48) Coradin, T.; Durupthy, O.; Livage, J. *Langmuir* **2002**, *18*, 2331–2336.
(49) Coradin, T.; Livage, J. *Colloids Surf., B* **2001**, *21*, 329–336.
(50) Desimone, M. F.; Hélary, C.; Rietveld, I. B.; Bataille, J.; Mosser, G.; Giraud-Guille, M.-M.; Livage, J.; Coradin, T. *Acta Biomater.* **2010**, *6*, 3998–4004.
(51) Annenkov, V. V.; Patwardhan, S. V.; Belton, D.; Danilovtseva, E. N.; Perry, C. C. *Chem. Commun.* **2006**, 1521–1523.
(52) Patwardhan, S. V.; Clarson, S. J.; Perry, C. C. *Chem. Commun.* **2005**, 1113–1121.
(53) Belton, D. J.; Patwardhan, S. V.; Annenkov, V. V.; Danilovtseva, E. N.; Perry, C. C. *Proc. Natl. Acad. Sci. U.S.A.* **2008**, *105*, 5963–5968.
(54) Scheffel, A.; Poulsen, N.; Shian, S.; Kröger, N. *Proc. Natl. Acad. Sci. U.S.A.* **2011**, *108*, 3175–3180.
(55) Sumper, M. *Angew. Chem., Int. Ed.* **2004**, *43*, 2251–2254.
(56) Sumper, M.; Lorenz, S.; Brunner, E. *Angew. Chem., Int. Ed.* **2003**, *42*, 5192–5195.
(57) Wenzl, S.; Hett, R.; Richthammer, P.; Sumper, M. *Angew. Chem., Int. Ed.* **2008**, *47*, 1729–1732.
(58) Brunner, E.; Lutz, K.; Sumper, M. *Phys. Chem. Chem. Phys.* **2004**, *6*, 854–857.
(59) Lutz, K.; Gröger, C.; Sumper, M.; Brunner, E. *Phys. Chem. Chem. Phys.* **2005**, *7*, 2812–2815.
(60) Annenkov, V. V.; Danilovtseva, E. N.; Pal'shin, V. A.; Aseyev, V. O.; Petrov, A. K.; Kozlov, A. S.; Patwardhan, S. V.; Perry, C. C. *Biomacromolecules* **2011**, *12*, 1772–1780.
(61) Danilovtseva, E. N.; Pal'shin, V. A.; Likhoshway, Y. V.; Annenkov, V. V. *Adv. Sci. Lett.* **2011**, *4*, 616–621.
(62) Neofotistou, E.; Demadis, K. D. *Colloids Surf., A* **2004**, *242*, 213–216.
(63) Demadis, K. D.; Neofotistou, E. *Chem. Mater.* **2007**, *19*, 581–587.
(64) Mavredaki, E.; Neofotistou, E.; Demadis, K. D. *Ind. Eng. Chem. Res.* **2005**, *44*, 7019–7026.
(65) Demadis, K. D. *J. Chem. Technol. Biotechnol.* **2005**, *80*, 630–640.
(66) Demadis, K. D.; Stathoulopoulou, A. *Ind. Eng. Chem. Res.* **2006**, *45*, 4436–4440.
(67) Demadis, K. D.; Neofotistou, E.; Mavredaki, E.; Tsiknakis, M.; Sarigiannidou, E.-M.; Katarachia, S. D. *Desalination* **2005**, *179*, 281–295.
(68) Mavredaki, E.; Stathoulopoulou, A.; Neofotistou, E.; Demadis, K. D. *Desalination* **2007**, *210*, 257–265.
(69) Demadis, K. D.; Ketsetzi, A.; Pachis, K.; Ramos, V. M. *Biomacromolecules* **2008**, *9*, 3288–3293.
(70) Demadis, K. D.; Pachis, K.; Ketsetzi, A.; Stathoulopoulou, A. *Adv. Colloid Interface Sci.* **2009**, *151*, 33–48.
(71) (a) Bai, S.; Tsuji, Y.; Okaue, Y.; Yokoyama, T. *Chem. Lett.* **2008**, *37*, 1168–1169. (b) Bai, S.; Okaue, Y.; Yokoyama, T. *Polym. Degrad. Stab.* **2009**, *94*, 1795–1799. (c) Bai, S.; Tsuji, Y.; Okaue, Y.; Yokoyama, T. *J. Solution Chem.* **2011**, *40*, 348–356.
(72) Helmecke, O.; Hirsch, A.; Behrens, P.; Menzel, H. *J. Colloid Interface Sci.* **2008**, *321*, 44–51.
(73) Patwardhan, S. V.; Clarson, S. J. *Silicon Chem.* **2002**, *1*, 207–214.
(74) Patwardhan, S. V.; Mukherjee, N.; Clarson, S. J. *Silicon Chem.* **2002**, *1*, 47–57.
(75) Patwardhan, S. V.; Clarson, S. J. *Mater. Sci. Eng., C* **2003**, *23*, 495–499.
(76) (a) Mizutani, T.; Nagase, H.; Fujiwara, N.; Ogoshi, H. *Bull. Chem. Soc. Jpn.* **1998**, *71*, 2017–2022. (b) Mizutani, T.; Nagase, H.; Ogoshi, H. *Chem. Lett.* **1998**, *2*, 133–134.
(77) Hsiao, C. N.; Huang, K. S. *J. Appl. Polym. Sci.* **2005**, *96*, 1936–1942.
(78) Behrens, P.; Baeuerlein, E. *Handbook of Biomineralisation—Biomimetic and Bioinspired Chemistry*; Wiley: Weinheim, Germany, 2007; pp 10−12.
(79) Menzel, H.; Horstmann, S.; Behrens, P.; Bärnreuther, P.; Krueger, I.; Jahns, M. *Chem. Commun.* **2003**, 2994–2995.
(80) Knecht, M. R.; Sewell, S. L.; Wright, D. W. *Langmuir* **2005**, *21*, 2058–2061.
(81) Knecht, M. R.; Wright, D. W. *Chem. Mater.* **2004**, *16*, 4890–4895.
(82) Brauer, G. *Das Handbuch der Präperativen anorganischen Chemie*; Enke Verlag: Stuttgart, Germany, 1975.
(83) Fung, B. M.; Khitrin, A. K.; Ermolaev, K. *J. Magn. Reson.* **2000**, *142*, 97–101.
(84) Massiot, D.; Fayon, F.; Capron, M.; King, I.; Le Calvé, S.; Alonso, B.; Durand, J. O.; Bujoli, B.; Gan, Z.; Hoatson, G. *Magn. Reson. Chem.* **2002**, *40*, 70–76.
(85) Amjad, Z.; Zuhl, B. *Mater. Perform.* **2009**, *48*, 48–52.
(86) Ketsetzi, A.; Stathoulopoulou, A.; Demadis, K. D. *Desalination* **2008**, *223*, 487–493.
(87) (a) Vrieling, E. G.; Beelen, T. P. M.; Gieskes, W. W. C. *J. Phycol.* **1999**, *35*, 548–559. (b) Vrieling, E. G.; Beelen, T. P. M.; van Santen, R. A.; Gieskes, W. W. C. *Angew. Chem., Int. Ed.* **2002**, *41*, 1543–1546. (c) Hazelaar, S.; van der Strate, H. J.; Gieskes, W. W. C.; Vrieling, E. G. *J. Phycol.* **2005**, *41*, 354–358. (d) Gordon, R.; Drum, R. W. *Int. Rev. Cytol.* **1994**, *150*, 243–372.
(88) (a) Abendroth, R. P. *J. Colloid Interface Sci.* **1970**, *34*, 591–596. (b) Bolt, G. H. *J. Phys. Chem.* **1957**, *61*, 1166–1169. (c) Sposito, G. J. *J. Colloid Interface Sci.* **1983**, *91*, 329–340. (d) Schindler, P.; Kamber, H. R. *Helv. Chim. Acta* **1968**, *51*, 1781–1786. (e) Zhuravlev, L. T. *Colloids Surf., A* **1993**, *74*, 71–90. (f) Abendroth, R. P. *J. Phys. Chem.* **1972**, *76*, 2547–2549. (g) Zhuravlev, L. T. *Colloids Surf., A* **2000**, *173*, 1–38.
(89) (a) Simonutti, R.; Comotti, A.; Negroni, F.; Sozzani, P. *Chem. Mater.* **1999**, *11*, 822–828. (b) Simonutti, R.; Comotti, A.; Bracco, S.; Sozzani, P. *Chem. Mater.* **2001**, *13*, 771–777. (c) Comotti, A.; Bracco, S.; Valsesia, P.; Ferretti, L.; Sozzani, P. *J. Am. Chem. Soc.* **2007**, *129*, 8566–8576. (d) Valsesia, P.; Beretta, M.; Bracco, S.; Comotti, A.; Sozzani, P. *J. Mater. Chem.* **2008**, *18*, 5511–5517.
(90) Robinson, S.; Williams, P. A. *Langmuir* **2002**, *18*, 8743–8748.
(91) Belyakova, L. A.; Varvarin, A. M.; Lyashenko, D. Y.; Roik, N. V. *J. Colloid Interface Sci.* **2003**, *264*, 2–6.
(92) (a) Gun'ko, V. M.; Voronin, E. F.; Zarko, V. I.; Goncharuk, E. V.; Turov, V. V.; Pakhovchishin, S. V.; Pakhlov, E. M.; Guzenko, N. V.; Leboda, R.; Skubiszewska-Zieba, J.; Janusz, W.; Chibowski, S.; Chibowski, E.; Chuiko, A. A. *Colloids Surf., A* **2004**, *233*, 63–78. (b) Gun'ko, V. M.; Voronin, E. F.; Nosach, L. V.; Pakhlov, E. M.; Voronina, O. E.; Guzenko, N. V.; Kazakova, O. A.; Leboda, R.; Skubiszewska-Zieba, J. *Appl. Surf. Sci.* **2006**, *253*, 2801–2811.
(93) (a) Goncharuk, E. V.; Pakhovchishin, S. V.; Zarko, V. I.; Gun'ko, V. M. *Colloid J.* **2001**, *63*, 283–289. (b) Gun'ko, V. M.; Zarko, V. I.; Turov, V. V.; Goncharuk, E. V.; Voronin, E. F.; Kazakova, O. A. *Theor. Exp. Chem.* **2001**, *37*, 75–79. (c) Gun'ko, V. M.; Zarko, V. I.; Voronin, E. F.; Turov, V. V.; Mironyuk, I. F.; Gerashchenko, I. I.; Goncharuk, E. V.; Pakhlov, E. M.; Guzenko, N. V.; Leboda, R.; Skubiszewska-Zieba, J.; Janusz, W.; Chibowski, S.; Levchuk, Yu. N.; Klyueva, A. V. *Langmuir* **2002**, *18*, 581–596. (d) Kazakova, O. A.; Gun'ko, V. M.; Lipkovskaya, N. A.; Voronin, E. F.; Pogorelyi, V. K. *Colloid J.* **2002**, *64*, 412–418.
(94) Xu, Y.; Wu, D.; Sun, Y.; Chen, W.; Yuan, H.; Deng, F.; Wu, Z. *Colloids Surf., A* **2007**, *305*, 97–104.
(95) (a) Demadis, K. D.; Neofotistou, E. *Desalination* **2004**, *167*, 257–272. (b) Demadis, K. D.; Mavredaki, E.; Stathoulopoulou, A.; Neofotistou, E.; Mantzaridis, C *Desalination* **2007**, *213*, 38–46.
(96) Bielecki, A.; Kolbert, A. C.; Levitt, M. H. *Chem. Phys. Lett.* **1989**, *155*, 341–346.

(97) Perrino, M. P.; Navarro, R.; Tardajos, M. G.; Gallardo, A.; Reinecke, H. *Macromol. Chem. Phys.* **2009**, *210*, 1973–1978.
(98) Stöber, W.; Fink, A.; Bohn, E. *J. Colloid Interface Sci.* **1968**, *26*, 62–68.
(99) Fotou, G. P.; Pratsinis, S. E.; Pinto, N. G. *J. Non-Cryst. Solids* **1995**, *183*, 135–143.
(100) Benmouhoub, N.; Simmonet, N.; Agoudjil, N.; Coradin, T. *Green Chem.* **2008**, *10*, 957–964.
(101) Yang, Y.; Coradin, T. *Green Chem.* **2008**, *10*, 183–190.
(102) Ehrlich, H.; Demadis, K. D.; Pokrovsky, O. S.; Koutsoukos, P. G. *Chem. Rev.* **2010**, *110*, 4656−4689, and references therein.